FURTHER RESULTS ON NUMERICAL CLOUD SEEDING SIMULATIONS OF STRATIFORM-TYPE CLOUDS

Harold D. Orville, John H. Hirsch and Richard D. Farley
Institute of Atmospheric Sciences
South Dakota School of Mines and Technology
Rapid City, South Dakota 57701-3995

Abstract. Numerical simulations of ice-phase seeding of stratiform-type clouds have revealed the possibility of producing embedded convective cells in a stably stratified cloudy atmosphere. The requirements for this to occur are a high production rate of ice crystals from the seeding agent and a relatively low diffusion rate of the agent. The physical effect of the seeding is to glaciate a region of the cloud and cause the cloudy atmosphere to change from a saturated state with respect to liquid water to one saturated with respect to ice. Such a transformation releases heat of deposition, causing a few tenths of a degree increase in temperature and a few m s^{-1} increase in vertical velocity. The transformation also produces one to two tenths of a gram of cloud ice per kilogram of air. These results have implications for convective clouds also. The temperature changes may help explain the often quoted positive impact of cloud seeding on moderate size convective clouds. Convective clouds in the range from 2 to almost 6 km depth show the largest potential for dynamic growth. These depths normally cover the -10°C to -25°C levels in the atmosphere, the temperature range of maximum effects for the transformation from saturation with respect to water (liquid) to one with respect to ice.

1. INTRODUCTION

In the December 1984 issue of the Journal of Climate and Applied Meteorology, Orville et al. (1984) (hereafter referred to as OFH) present results of the simulated seeding of a stratiform-type cloud. Explosive growth of a cumulus cell embedded in a nimbostratus model cloud is demonstrated. Considerable convective development at the top of the stratiform layer is present in both the seeded and unseeded simulations due to the unstable upper atmosphere represented in the atmospheric sounding used to initiate the model runs. This raises questions about the necessity of the upper layer to the stimulated growth of the embedded cells created by the cloud seeding.

To answer these questions, we have rerun the cloud model with the upper convective layer replaced by a stable layer. Consequently, the stratiform layer deepens with time, but no convective cells are produced at the cloud top and there is no explosive growth of cells to 10 km or higher, as is depicted in the journal article. Still embedded convection develops in the moist, adiabatic stratiform layer. Brief descriptions of these new results are presented below.

In addition to these results, we have done further calculations regarding the latent heat release when "very dry" clouds switch from saturation with respect to liquid water to saturation with respect to ice. These calculations cover a range of conditions which are at lower temperatures than in the OFH article. The calculations show even greater temperature increases than the 0.2°C to 0.3°C changes evident in OFH, as great as 0.68°C at 400 hPa and -20°C in these recent calculations.

The implications of such temperature changes are significant; the increases may be important in anvil clouds, which are not necessarily all ice, for stratiform precipitation from mesoscale convective systems, and for creating convective cells in upper layer cirrostratus layers [as observed by Sassen et al. (1985) and suggested by Johnson and Kriete (1982)].

The cloud model used in the study is two-dimensional and time dependent. Bulk water microphysics involving cloud water, cloud ice, snow, graupel/hail, and rain are used (Lin et al., 1983). To produce the layer cloud, mesoscale convergence is superimposed in the lower levels with divergence aloft (Chen and Orville, 1980). The seeding simulation techniques are described in Hsie et al. (1980) and in OFH. We use a uniform grid interval of 200 m in both the horizontal and vertical directions over a domain of about 20 km on a side.

2. BRIEF DESCRIPTION OF THE SEEDING RESULTS

Figures 1-4 illustrate the salient points from the model run with the modified atmospheric sounding (the layer from 500 hPa to 200 hPa has been changed from a lapse rate of 8.6°C/km to 6.0°C/km; see the OFH article for the original sounding).

Figure 1 shows the outline of the cloud, the streamlines, and the regions with snow content greater than 0.1 g kg^{-1} at 45 min of simulated real time. The seed case also shows the pattern of the initial silver iodide (AgI) release at 33 min. The simulations assumed about 100 g of AgI per km in the y-direction. See OFH for a description of the seeding simulations.

The main differences evident in the seed and no-seed cases are the regions of zero liquid water in the seeded cloud at about the 3 km to 4 km level, and at 5 km and 8 km in from the left boundary, and the slightly perturbed streamlines in these regions.

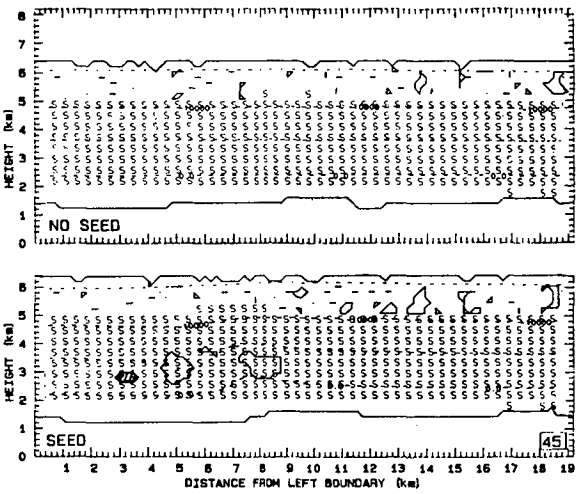

Fig. 1: Cloud outline at 45 min of simulated real time. The top frame shows the no-seed simulation; the bottom is the seed case. The S symbols denote snow content greater than 0.1 g kg^{-1}. Streamlines are dashed and indicate a speed of 5 m s^{-1} when spaced 1 km apart. Solid lines are the cloud outline where the R.H. is 100%.

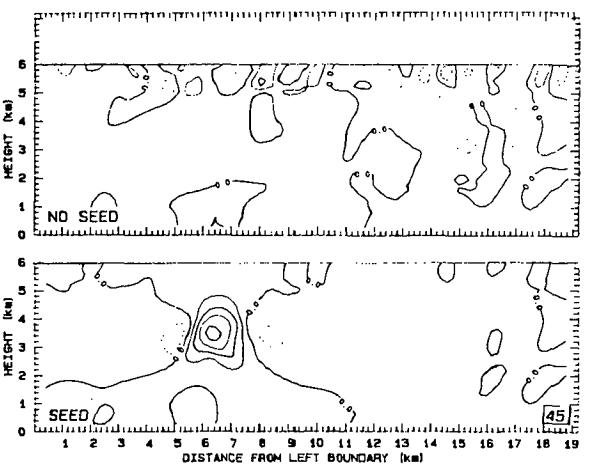

Fig. 2: Vertical velocity at 45 min of simulated real time. The top frame shows the no-seed simulation; the bottom is the seed case. The range in the top frame is from -0.28 to 0.22 m s^{-1} with a contour interval of 0.1 m s^{-1}; in the bottom frame, the range is from -1.6 to 4.3 m s^{-1} with a contour interval of 1 m s^{-1}.

Figure 2 shows the vertical velocity fields in the two cases at 45 min, 12 min after seeding. The seed case has a maximum updraft of 4.3 m s^{-1} in an embedded convective cell, which has been caused by the AgI seeding. The no-seed case has a maximum updraft of only 0.22 m s^{-1}.

Figure 3 shows one result of the augmented circulation. The liquid water content in the seed case is greatly increased in the embedded convective cell. Nearly 0.5 g kg^{-1} of supercooled liquid water has developed, some below and some above the convective cell. Less than 0.2 g kg^{-1} of water exists in the no-seed case. The temperature fields (not shown here) indicate a maximum temperature excess of just over 2°C in the convective cell.

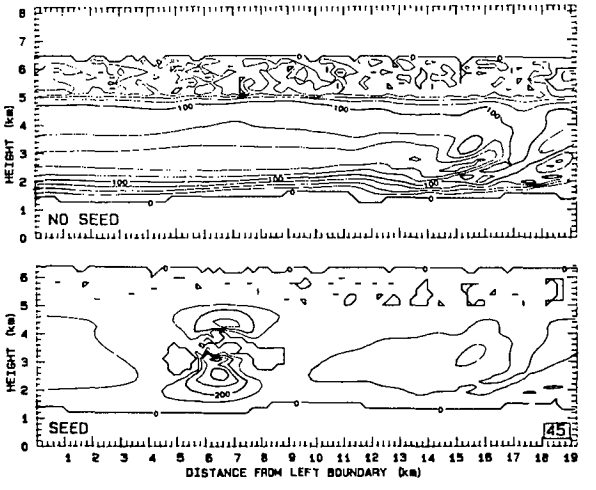

Fig. 3: Liquid water content at 45 min of simulated real time. Top frame shows the no-seed simulation; the bottom is the seeded case. The contour interval in the top frame is 2.5 x 10^{-5} g g^{-1}. The values range from 0 to 1.86 x 10^{-4} g g^{-1}. In the bottom frame, the contour interval is 1 x 10^{-4} g g^{-1}; the values range from 0 to 4.94 x 10^{-4} g g^{-1}.

The development of the convective cell and the reasons for the development follow the discussion given in OFH. The formation of cloud ice by the seeding at 33 min is followed by snow formation, the accretion of the supercooled water by the snow, and the drying out of the cloud. The heat release by the adjustment to saturation with respect to ice from saturation with respect to liquid is a significant portion of the heating. The excess temperature stimulates the vertical motion, leading to enhanced condensation and further convective development, but all within the stratiform layer. No upper level convection develops.

As in OFH, additional rain is produced and some redistribution occurs. Figure 4 shows the accumulated rain in the two cases after 69 min of real time simulation. A few tenths of a millimeter have accumulated on the ground.

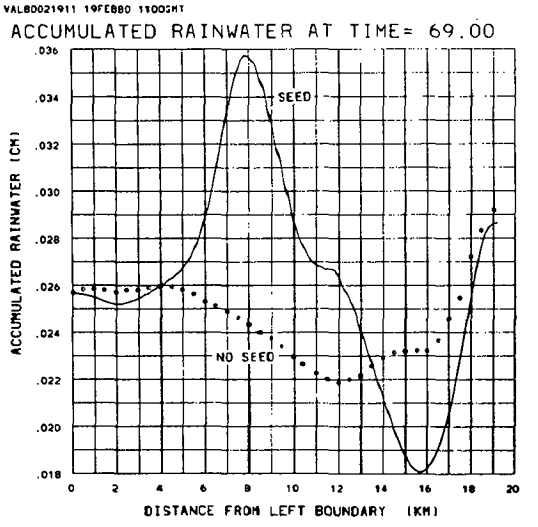

Fig. 4: Rain accumulation at the ground (cm) along the x-axis at 69 min. Solid line is the amount from the AgI seed simulation; the dotted curve is that of the no-seed simulation.

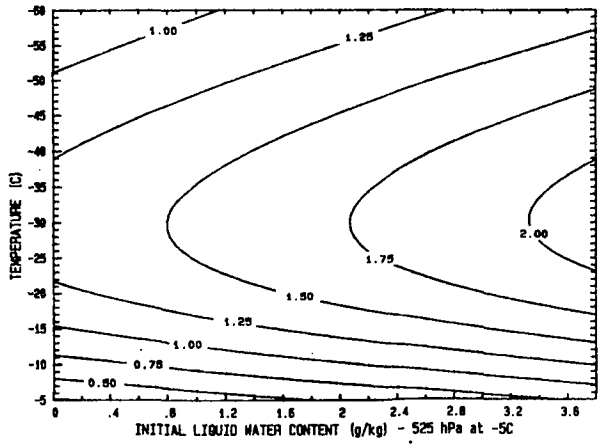

Fig. 5: Contour plot of temperature changes within a parcel due to freezing liquid water at specified initial conditions of water content and temperature. Parcel ascent begins at 525 hPa at -5°C.

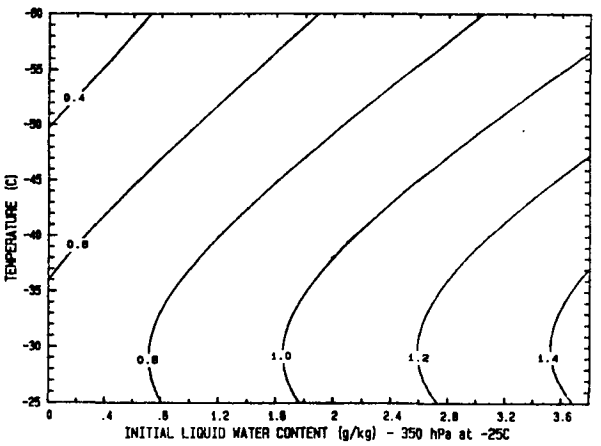

Fig. 6: Same as Fig. 5, but parcel ascent begins at 350 hPa at -25°C.

3. CALCULATIONS OF THE HEAT RELEASE DUE TO FREEZING

Orville and Hubbard (1973) give results of temperature changes that occur when transforming from liquid to ice in a rising parcel of air. Equations from Saunders (1957) were used to illustrate the effects. At the time, we were using the results to show that less heating is obtained than some scientists had thought from the freezing of fairly wet tropical clouds (those with a few to several g kg^{-1} of supercooled liquid water).

Figures 5 and 6 show results for freezing the liquid water in a parcel of air at specified initial conditions given in the figures and then raising the parcel along a saturated ice adiabat. The temperature differences shown are those between such a parcel and one that remains in an all liquid saturated adiabatic process.

Large temperature differences arise even at the very low liquid water content region of the graphs. More than 1°C temperature differences can occur if a relatively dry parcel rises from 525 hPa and -5°C; more than 2°C excess heating over that in a "water" parcel can occur if the initial liquid water mixing ratio is 3 g kg^{-1} or more.

The temperature excesses at the low end of the scale prompted us to calculate the changes for parcels switching from water saturation to ice saturation, at the limiting factor of zero liquid water mixing ratio. No rise of the parcel is assumed. In nature, parcels of 0.1 g kg^{-1} to 0.05 g kg^{-1} or less may remain at liquid saturation, in the absence of ice crystals. Also, when new condensation occurs it will more than likely form more cloud droplets because of the more numerous cloud condensation nuclei compared with the number of ice nuclei. Consequently, the normal atmospheric condition would appear to be water (liquid) saturation, leading to many opportunities to cause switches from liquid to ice saturation.

Figure 7 shows the results of the calculations for pressures of 400 and 600 hPa. In addition to the excess temperatures created, the figure shows the amount of cloud ice formed in the transformation from liquid to ice saturation.

Nearly 0.7°C temperature excess is produced at -15°C to -20°C and at 400 hPa. More than 0.2 g kg^{-1} of ice is produced in the process. These changes could have significant effects on the circulations within the clouds, leading to enhanced condensation and deposition and more precipitation formation. Observations of supercooled liquid and enhanced circulations at high altitudes may be due to such thermodynamic/dynamic interactions (see Sassen et al., 1985).

These results have implications for convective clouds also, and perhaps give further reasons for the efficacy of cloud seeding when applied to moderate size convective clouds. To see this, we look at results obtained in earlier studies from a one-dimensional, steady-state numerical cloud model applied to soundings from the North Dakota Cloud Modification Project (NDCMP). The model described by Hirsch (1971) is run for various assumed initial updraft sizes in both non-seeded and seeded versions to obtain estimates of the effect of seeding on the vertical growth of the clouds (as well as on updraft speed and other cloud characteristics). The difference, ΔH, between cloud top heights in the seeded and non-seeded versions of a model cloud can be taken as an indication of seedability, as suggested by Simpson et al. (1967).

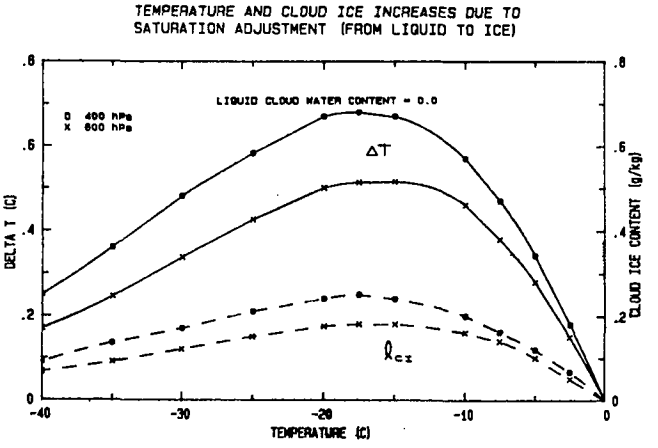

Fig. 7: Temperature (solid curves) and ice content (dashed curves) changes due to saturation adjustments at various temperatures. The curves were computed for 400 hPa (O's) and 600 hPa (X's).

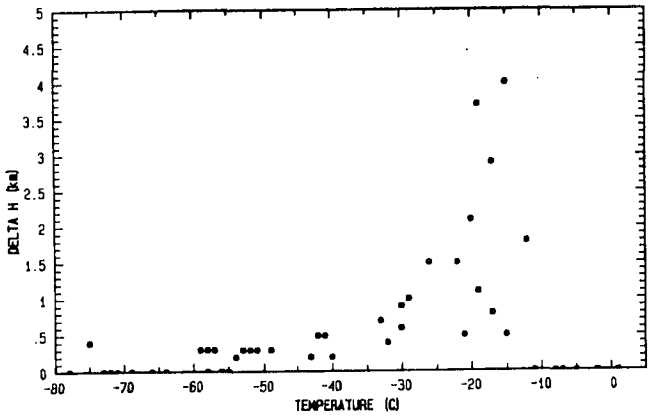

Fig. 8: Scatter plot comparing the computed increase in cloud top height (ΔH) due to seeding, for model clouds with 5 km updraft diameters, with the corresponding initial (i.e., unseeded) cloud-top temperature. One sounding for each day in 1982/84 was used. [Taken from Smith et al., 1986.]

Figure 8 shows a plot of this cloud top growth (ΔH) versus the initial (unseeded) cloud top temperature from the model, using data from the 1982 NDCMP. Obviously, substantial growth occurs for clouds with top temperatures (in the unseeded version of the model) mainly in the range -10°C to -20°C. That is the temperature range in which maximum heating effects due to the switch from liquid to ice saturation accompanying seeding would occur (Fig. 7).

This cloud model was also applied to all days during the 1972 NDPP. Figure 9 shows a graph of natural cloud model depths versus seeded model depths. The model suggests that the greatest potential for ice-phase cloud seeding response lies in the lower middle range of cloud sizes, peaking in clouds whose depths lie between 2.5 and 5.5 km and in the range of temperatures mentioned above.

Results from another one-dimensional cloud model show the same tendencies for extra growth in the middle size cloud range (Ackerman and Sun, 1985; their Fig. 2).

4. SUMMARY

Modeling results using a stable late winter sounding show that embedded convective cells can be produced in a supercooled stratiform layer. Temperature increases of several tenths of a degree Celsius and one or two tenths of a gram of ice per kilogram of air may be produced, due to the transformation from liquid saturation to ice saturation in very dry clouds (clouds with 0.1 g kg^{-1} liquid water mixing ratio or less). The heat of deposition is the cause of the temperature increases. Either artificial or natural seeding of supercooled cloud regions could produce these effects.

In addition, the often quoted dynamic effects of seeding on moderate size convective clouds may be partially explained by the extra heating and dynamic effects in the -10°C to -20°C range shown by the calculations.

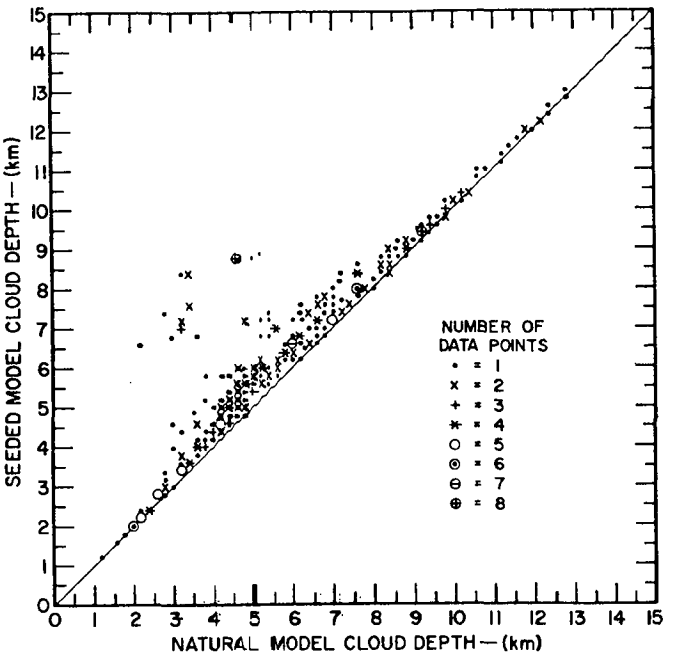

Fig. 9: Graph showing natural model cloud depths vs. seeded model cloud depths. Various symbols are used at points where multiple data points overlapped. The average increase in model cloud depth was 770 meters.

Acknowledgments. We thank Mrs. Joie Robinson and Miss Carol Vande Bossche for typing the manuscript and arranging the figures. Also we thank Miss Ling May Wu for preparing the Saunders' freezing graphs.

The work was supported by the National Science Foundation, Division of Atmospheric Sciences, under NSF Grant Nos. ATM-8311711 and ATM-8516940.

REFERENCES

Ackerman, B., and R. Y. Sun, 1985: Predictions by two one-dimensional cloud models: A comparison. J. Climate Appl. Meteor., 24, 617-628.

Chen, C. H., and H. D. Orville, 1980: Effects of mesoscale convergence on cloud convection. J. Appl. Meteor., 19, 256-274.

Hirsch, J. H., 1971: Computer modeling of cumulus clouds during Project Cloud Catcher. Report 71-7, Institute of Atmospheric Sciences, S.D. School of Mines and Technology, Rapid City, SD. 61 pp.

Hsie, E. Y., R. D. Farley and H. D. Orville, 1980: Numerical simulation of ice-phase convective cloud seeding. J. Appl. Meteor., 19, 950-977.

Johnson, R. J., and D. C. Kriete, 1982: Thermodynamic and circulation characteristics of winter monsoon tropical mesoscale convection. Mon. Wea. Rev., 110, 1898-1911.

Lin, Y. L., R. D. Farley and H. D. Orville, 1983: Bulk parameterization of the snow field in a cloud model. J. Climate Appl. Meteor., 22, 1065-1092.

Orville, H. D., R. D. Farley and J. H. Hirsch, 1984: Some surprising results from simulated seeding of stratiform-type clouds. J. Climate Appl. Meteor., 23, 1585-1600.

_____, and K. G. Hubbard, 1973: On the freezing of liquid water in a cloud. J. Appl. Meteor., 12, 671-676.

Sassen, K., K. N. Liou, S. Kinne and M. Griffin, 1985: Highly supercooled cirrus cloud water: confirmation and climatic implications. Science, 227, 411-413.

Saunders, P. M., 1957: The thermodynamics of saturated air: a contribution to the classical theory. Quart. J. Roy. Meteor. Soc., 83, 342-350.

Simpson, J., G. W. Brier and R. H. Simpson, 1967: Stormfury cumulus seeding experiment 1965: Statistical analysis and main results. J. Atmos. Sci., 24, 508-521.

Smith, P. L., J. R. Miller, Jr., J. H. Hirsch and H. D. Orville, 1986: Dynamic versus microphysical effects of seeding: Some cloud model and radar observations. Preprints 10th Conf. Planned and Inadvertent Wea. Modif., Arlington, VA, Amer. Meteor. Soc., 175-178.